

Gas Position Sensitive X-Ray Detectors

Ademarlaudo França Barbosa

**Centro Brasileiro de Pesquisas Físicas - CBPF/CNPq
Rua Dr. Xavier Sigaud, 150
22290-180 - Rio de Janeiro, RJ - Brasil**

ABSTRACT

The construction of Gas X-Ray Detectors used to count and localize X-Ray photons in one and two dimensions is reported. The principles of operation of the detectors are described, as well as the electronic modules comprised in the data acquisition system. Results obtained with detectors built at CBPF are shown, illustrating the performance of the Linear Position Sensitive Detectors.

Key-words: X-Ray Detectors; Position Sensitive; Bidimensional Localisation; MWPC; Delay Line; Data Acquisition.

INDEX

| | |
|--|-----------|
| I - Introduction | 3 |
| II - One Dimensional Position Sensitive Detector | 3 |
| 2.1 - Principle of Operation | 3 |
| 2.2 - The Delay Line | 5 |
| 2.3 - Associated Electronics | 6 |
| - Pre-amplifier | 8 |
| - Amplifier & Discriminator | 9 |
| - Time to Analog Converter | 10 |
| - External Delay | 10 |
| - Analog to Digital Converter | 10 |
| III - Two Dimensional Position Sensitive Detector | 11 |
| 3.1 - Multi-Wire Proportional Counters | 11 |
| 3.2 - The X&Y Cathode | 12 |
| 3.3 - Wire Weaving | 14 |
| 3.4 - Data Acquisition System | 14 |
| IV - Characterisation Measurements | 15 |
| 4.1 - Spatial Resolution | 15 |
| 4.2 - Linearity | 16 |
| 4.3 - Homogeneity | 18 |
| V - Conclusion | 22 |
| VI - Acknowledgements | 23 |
| VII - References | 23 |

I - INTRODUCTION

Gas Position Sensitive X-Ray Detectors are presently built at the Brazilian Center for Physics Research (CBPF). '*Position Sensitive*' stands for the fact that, besides counting single photons interacting with the gas atoms, these detectors are able to measure their position of incidence with some accuracy, in one or two dimensions.

A Detectors Laboratory has been implemented for the construction of one-dimensional Position Sensitive Detectors (PSD). This kind of detectors is used for scanning X-Ray scattering patterns in applications such as Small Angle X-Ray Scattering, Wide Angle X-Ray Scattering, Computerized Tomography, etc. Usually, in these applications, one detector is used to measure the intensity of X-Ray scattering on discrete points along a line. In these cases, the time taken to scan a scattering pattern tends to be long, specially if high position resolution and high counting statistics are required. The use of PSD's strongly reduces the experiment time, since all the the scattering points of a pattern are scanned almost simultaneously.

A two-dimensional PSD is under development. It will allow on-line storing of data corresponding to X-Ray images on the detector window. Among the different possible applications of this kind of detectors, the fast scanning of two-dimensional scattering patterns from samples should be pointed, in particular in cases where structural transformation occur in a short length of time.

In this report we describe the operation and construction of these detectors, as well as the electronic parts involved in their data acquisition systems.

II - ONE DIMENSIONAL POSITION SENSITIVE DETECTOR

2.1 - Principle of Operation

In the X-Ray range of energy (≈ 1 KeV to 100 KeV), the photo-electric effect is one of the most likely interactions to take place between photons and matter. The photo-electron resulting from this interaction is the origin of the 'signal' to be observed after the passage of a photon through a detecting medium. It loses its energy by ionizing atoms of the medium, generating other electrons with lower energies. Thus, the absorption of an X-Ray photon produces an amount of electric charge that could be collected at an electrode.

The detector consists essentially in a gas chamber where electrodes are provided in order to establish an electric field that drives electrons to a charge collecting circuit. The geometry of the electrodes is optimised in some features, such that the measurement of the position of incoming photons is made possible. One of these features is the anode wire, which is set to a high electric potential (≈ 2 Kilo-Volts). Since the electric field at a point around a cylindrical wire is inversely proportional to the radial distance, very high values of electric field are attained close to the wire surface. This field accelerates the electrons towards the wire. The accelerated electrons generate other electrons in shocks with gas molecules along their path. This phenomenon is known as 'avalanche'. It produces a high density of charge in a small region close to the wire surface, thus providing the spatially localized information needed in the position measurement. When the magnitude of the electric field is such that the avalanche charge is linearly proportional to the energy of the incident photon, the detector is said to operate in the 'proportional' mode.

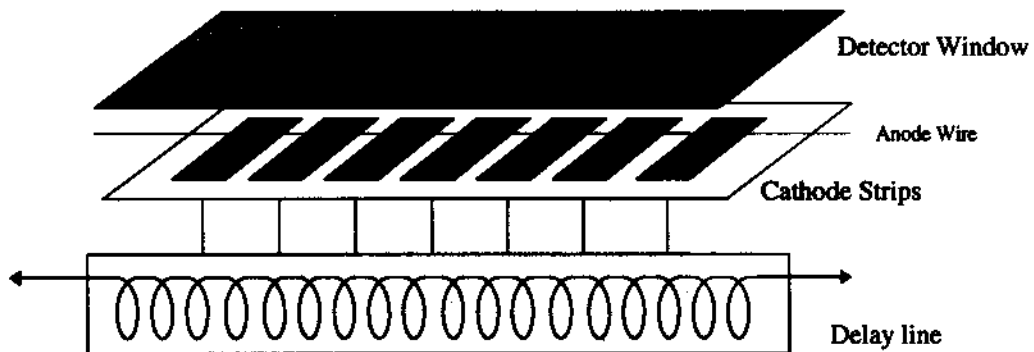


Fig. 01: Scheme of the detecting cell

The avalanche charge induces a charge distribution on the cathode surface, which is a flat electrode subdivided in conducting strips (See Fig. 01). The detector window plays the role of a cathode which, together with the other cathode plane, confines the anode wire approximately as in a geometry of coaxial cylinders.

The cathode strips are connected to a delay line, just as sketched in Fig. 01. The signal induced in the strips by an avalanche is then driven through the delay line, and the position of the incoming photon may be estimated from the time taken by the signal to reach the ends of the line [1].

2.2 The Delay Line

In order to measure the position of a photon producing an avalanche on the anode wire with best accuracy, we would expect the delay line not to introduce any distortion to the shape of the signal. This implies: no loss in amplitude and no distortion in its time development. Ideally, the delay line should faithfully reproduce the input signal at the output.

We can see briefly that these requirements can only approximately be satisfied. Let us take $A(t)$ to represent the amplitude of the signal as a function of time. We can look at it in the frequency domain, and consider one of its individual spectral components:

$$A_{in}(\omega) = A_0 \sin(\omega.t) .$$

The ideal delay line would respond to this input with the same wave form, introducing only a phase shift, ϕ , to account for the delay:

$$A_{out}(\omega) = A_0 \sin(\omega.t - \phi) = A_0 \sin[\omega.(t - \phi/\omega)] .$$

We see that the output spectral component is delayed of ϕ/ω with respect to the input. If the signal is not to be distorted, each spectral component should have the phase shift ϕ linearly proportional to its frequency, such that the delay is the same for all of them.

The delay time is comparable to (or greater than) the time duration of the input signal. Consequently, reflections of the input signal may not be neglected and the delay line must be terminated with some circuit of impedance as close as possible to the characteristic impedance of the line.

If we take the delay line as being a perfect co-axial cable - that is, a cable with conductors featuring no resistivity - and consider only its capacitance (C) and auto-inductance (L) per unit length, we can demonstrate that the following expression is valid for any spectral component of the signal:

$$A_{out}(\omega) = A_{in}(\omega) . \text{Exp}(-i.\phi) ,$$

where,

$$\phi = \text{ArcCos}(1 - \vartheta^2) \quad [\vartheta < 1] ,$$

$$\vartheta = \omega/\omega_c ,$$

$$\omega_c^2 = L/C .$$

ω_c is a critical frequency above which the cable attenuates the spectral components. It is assumed that the cable is perfectly terminated.

Although the output preserves the amplitude of the input spectral components, it is clear that the phase shift φ is not a linear function of the frequency. However, if we neglect higher order terms in the series expansion of φ in terms of ϑ , we find that:

$$\varphi(\omega) \approx 2 \cdot \vartheta = 2 \cdot \omega / \omega_c .$$

We can conclude that the delay line is likely to transfer almost ideally the spectral components of a signal, provided that their frequencies are much lower than ω_c .

In the construction of the delay line, we use discrete L and C components in cascade (See Fig. 02). Each L-C cell is connected to one cathode strip. The limitations discussed above are taken into account by choosing L and C so that ω_c is high enough not to disturb critically the signal propagation.

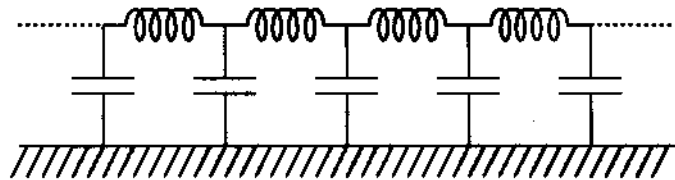


Fig. 02: Delay line circuit.

2.3 Associated Electronics

The characteristics of the signal observed in the detector for each absorbed photon may be estimated from the description given in Section 2.1. Let us consider photons in the range of 10^3 eV. The photo-electron has greater probability to be ejected from a K-shell of the atoms in the gas (usually Argon), where the binding energy is around 30 eV. Assuming that the photo-electron loses all its energy in collisions with gas molecules, which in turn eject new electrons, a maximum number of $\approx 10^3$ eV / 30 eV electrons is generated after the absorption of the photon. These primary electrons are multiplied by a factor as large as $10^3 - 10^4$, due to the avalanche phenomenon mentioned above.

Since the geometry of the electrodes in the detector produces a capacitance (C_0) of a few pico-Farads, the total charge ($\delta q \approx 10^{-15}$ Coulomb) collected entails a potential variation:

$$\delta V = \delta q / C_0 \approx 10^{-3} \text{ Volt} .$$

The time development of this potential variation depends on the mobility of electrons and positive ions in the gas under the electric field [2]. Since the mass of an electron is $\approx 10^3$ times smaller than the mass of a positive ion, the electrons reach the anode wire much faster than the positive ions reach the cathode. This defines a potential variation of fast rise-time (electrons being collected in some nano-seconds), followed by a slower asymptotical raise up to to the final amplitude (positive ions being collected in micro-seconds).

The considerations above refer to the signal at the electrodes of the detector. Actually, the signal concerning the position measurement is that arriving at the ends of the delay line. The complete circuit producing this one is equivalent to the R-C circuit shown in Fig. 03, where C represents the detector capacitance and R represents the characteristic impedance of the delay line. This circuit acts as a differentiator. It differentiates more or less efficiently, depending on the magnitude of the RC time constant as compared to the time development of the passing signal. When RC tends to infinity (much greater than the time duration of the signal) the differentiation is ineffective and one gets the whole signal profile at the delay line output. When RC tends to zero (much smaller than the time duration of the signal), the output is a fast pulse corresponding to the time derivative of the signal shape. Since the detector deals with a timing measurement to be associated with the photon position, the latter case is preferred. On the other hand, the differentiation may attenuate the signal amplitude, so that a compromise timing constant has to be chosen for a given signal to noise ratio.

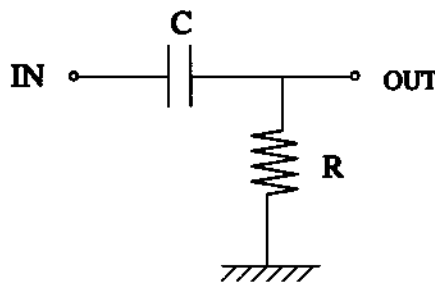


Fig. 03: Equivalent circuit for detector + delay line

After travelling through the delay line, the signal is treated by some electronic circuitry necessary to translate the detector internal phenomena to the expected information about the photon's incidence position. Fig. 04 represents these electronic parts, as described below.

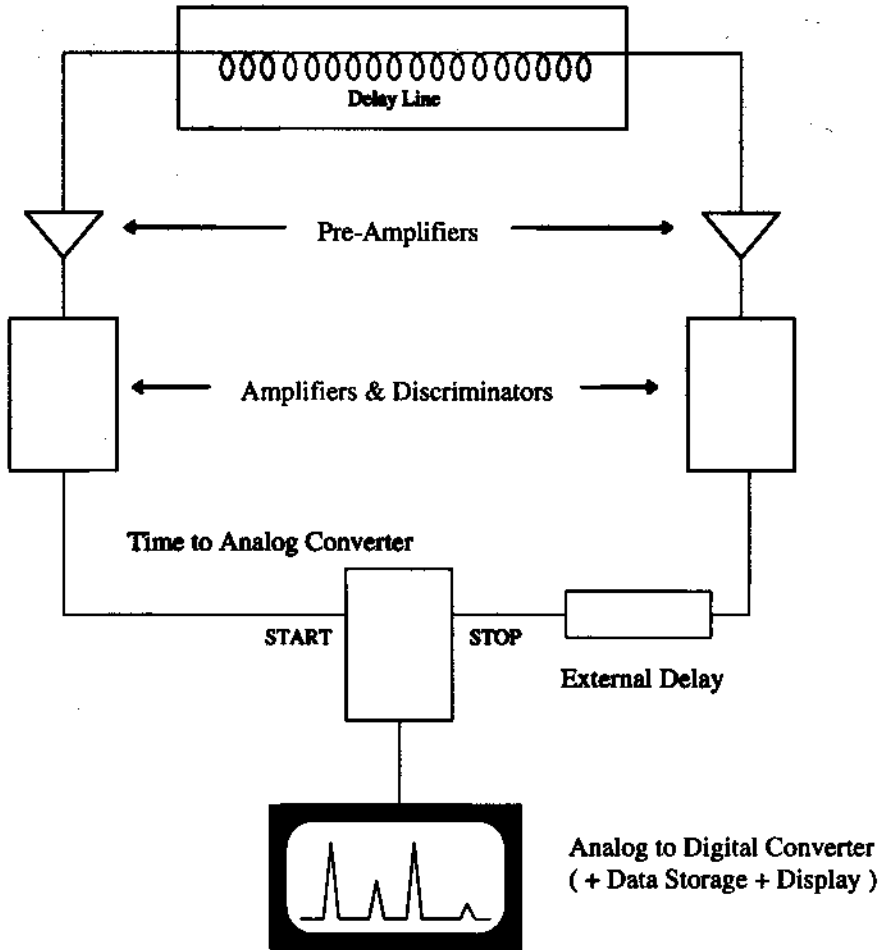


Fig. 04: Electronic parts composing the Data Acquisition System

- Pre-amplifier

As discussed above, the amplitude of the pulses at the output of the delay line is in the range of 10^{-3} Volts. The first role of the pre-amplifier is to amplify the signal to a range of amplitudes compatible with standard electronic modules. It also represents some load at the terminations of the delay line, which implies that its input impedance must be matched to the characteristic impedance of the line. The band-pass of the pre-amplifier and delay line must also be matched to the spectral components of the signal, so that it is passed with little distortion. These requirements call for special attention on the pre-amplifier circuit design. In practice we are led to build the pre-amplifier as a part of the detector.

- Amplifier & Discriminator

In order to define a precise timing criterium, it is often necessary to amplify the signal coming from the pre-amplifier. This may be accomplished by commercially available amplifier & shaping modules. The simplest timing technique consists in providing a circuit which compares the signal amplitude to a pre-set amplitude above the electronic noise. Whenever a photon is detected, the amplitude at the circuit input is higher than the pre-set value and a fast logic pulse is generated, which will be used for the time measurement (See 'Time to Analog Converter'). This kind of circuit is called Discriminator, since it distinguishes signal from electronic noise. The simple technique here described suffers from the drawback that the timing criterium depends on the signal amplitude, as shown in Fig. 05.

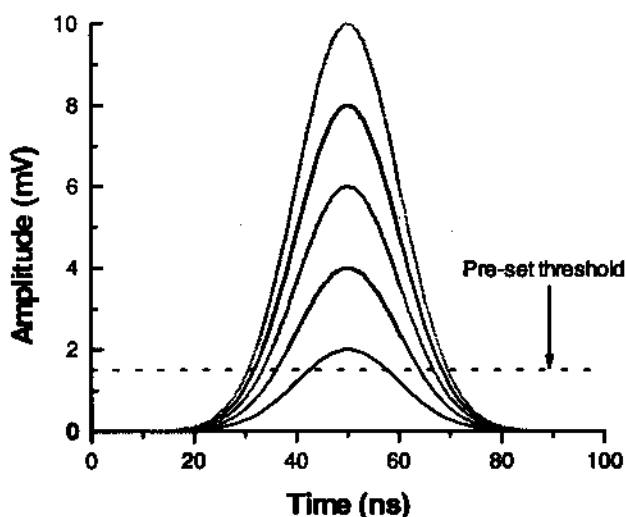


Fig. 05: Simple discrimination of signals differing in amplitude

It is seen in Fig. 05 that signals of different amplitudes occurring at the same time would trigger the fast logic pulse at different times. The consequence is that the time (\approx position) measurement will not be accurate. The drawback is accounted for in the so-called 'Constant Fraction Discriminators', where the output pulse is generated when the signal amplitude reaches a defined fraction of its maximum amplitude. In this case, the technique consists roughly in differentiating the input signal and generating the fast logic pulse at the zero-crossing time of its derivative.

- Time to Analog Converter

As seen in Section 2.1, the time taken by the avalanche signal to travel the to ends of the delay line can be directly associated to the position of the

photon causing the avalanche. The Time to Analog Converter is a standard electronic module which takes the logic pulses from the discriminators ('start' and 'stop') and outputs another pulse of amplitude proportional to their time difference. Usually, the 'start' pulse begins the charging up of a capacitor and the 'stop' pulse ends it. An output signal is generated with amplitude proportional to the charge stored in the capacitor. The position information is therefore contained in the amplitude of the signal at the output of the Time to Analog Converter.

- External Delay

The Time to Analog Converter can not handle situations where the 'stop' pulse arrives before the 'start'. In order to assure that a 'stop' pulse always arrives after the 'start', an external delay is generally used. Standard delay modules are commercially available. Delay circuits may be designed using simple TTL logic gates (eg. 74LS121).

- Analog to Digital Converter (ADC)

The final step in the translation of the detector's internal phenomena into position information consists in digitizing the output signal of the Time to Analog Converter. ADC's are largely used in physics laboratories, and are available under different electronic standards. In the present case, an ADC card is used which interfaces directly an IBM PC compatible bus. The digitized data are histogrammed in memory and displayed in a video monitor. Data are displayed simultaneously to the detector operation up to counting rates in the range of 10^4 - 10^5 counts/second. Higher count rates cause piling up of events processing, and the linearity between the counting rate and the photon flux at the detector is lost.

It should be noted that two conversion operations are done in the signal processing: Time to Analog and Analog to Digital. The conversion time is an ultimate limit to the counting rate. Direct Time to Digital Converters (TDC) are used in applications where high counting rates ($\approx 10^6$ counts/second) must be supported. Commercial and laboratory TDC's have been developed for these applications, generally based on the use of fast clocks (> 100 Mhz) to provide the time units.

III - TWO DIMENSIONAL POSITION SENSITIVE DETECTOR

3.1 - Multi-Wire Proportional Counters

The technique used to localize photons in the one-dimensional PSD may be readily extended to provide two dimensional localization. Section II describes the procedure to measure the photon position along a wire (say, the X coordinate). An immediate solution to the problem of finding the second coordinate consists in taking a set of parallel wires distributed regularly on a plane (Fig. 06): the Y coordinate in this case may be associated to the position of the wire collecting the avalanche.

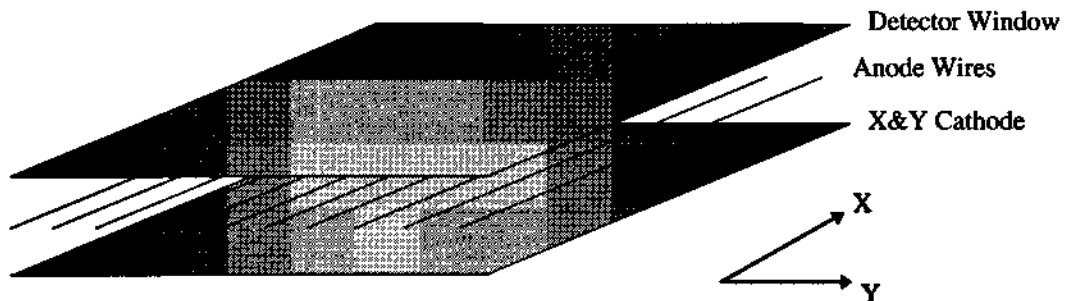


Fig. 06: Detecting cell for two dimensional PSD

The scheme shown in Fig. 06 has been originally proposed for applications in High Energy Physics [3]. Detectors based on it are called Multi-Wire Proportional Counters. In the present case, it is used for two-dimensional localization of X-Ray photons.

In the one-dimensional PSD, the delay line method is used to read out the X-coordinate from the charge induced by the avalanches on the conducting strips of the cathode. In order to preserve the same method for both coordinates, we have developed an X&Y cathode whose surface contains individual isolated conductors for sampling the induced charge in two-dimensions.

3.2 The X&Y Cathode

The evaluation of the amount of charge induced in the X&Y plane due to the presence of avalanche charge in one of the wires may be carried out from electrostatic considerations. In the absence of avalanche charge, some electric charge is distributed on the surface of the electrodes (detector window, anode wires and cathode), so that their electrostatic potential is hold constant. The presence of avalanche charge adds a contribution, V_q , to this potential. The charge induced by this contribution at a point (x,y) of the cathode surface, S , is given by:

$$\sigma(x, y) = -\epsilon \left[\frac{\partial V_q}{\partial z} \right]_S ,$$

where ϵ is the dielectric constant of the detecting medium and z is the direction orthogonal to the X&Y plane. The total charge induced in the whole cathode plane is thus:

$$q_{ind} = \int_S \sigma(x, y) dS .$$

In the case of a localized avalanche charge in the region between two cathode planes (neglecting the presence of anode wires), the full width at half maximum of the function $\sigma(x,y)$ is about 1.6 times [4,5] the distance between the avalanche charge and the cathode. A minimum number (> 2) of X&Y cathode elements is necessary for the sampling of the induced charge - otherwise, blind regions would be present in the detector response. If w is the pitch of the cathode elements in each direction and d is the distance between the avalanche and the X&Y cathode, this condition implies $w < 0.8d$.

The avalanche charge may be considered to be localized at the surface of one anode wire, and some charge is also induced in the neighbouring wires. Since the position readout is achieved from the charge induced in the X&Y cathode, an optimum geometry should be found for the electrodes configuration, so that most of the charge is induced on the cathode surface. Clearly, the X&Y cathode should preferably be placed as close as possible to the avalanche region, which might result in an anode-cathode distance (d) smaller than the anode wire pitch (s). In this case ($s > d$), one obtains a high resolution in the X direction, but a relatively poor position resolution for the Y-coordinate, since it is roughly measured in units of the wire pitch. A compromise has to be established for the electrodes configuration, such that an acceptable position resolution is obtained in both directions.

These considerations lead to two main guide-lines in the choice of the electrodes' geometry:

$$s \approx d ,$$

$$w < 0.8 d .$$

The X&Y cathode is composed of conducting pads distributed on a plane surface. It is implemented in a printed circuit board, as shown schematically in Fig. 07. Use is made of the multi-layer deposition technique, in order to provide the connection of two independent sets of pads to two groups of strips associated to the X & Y directions. The first (upper) layer contains only the conducting pads. Half of these pads is connected to a group of parallel strips in the second layer. The other half is connected to another group of parallel strips in the third layer, orthogonal to the first one. The connection of pads to strips is done through metalized holes crossing from the center of each pad to the corresponding strips.

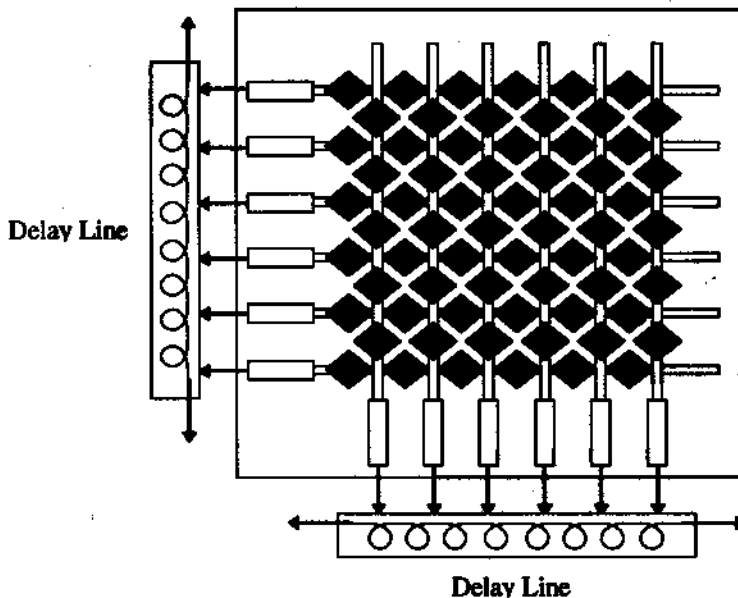


Fig. 07: Schematic view of the X&Y cathode

The pitch of the pads in each direction is 2.54 mm ($= w$). This parameter imposes, according to the condition discussed above, an anode-cathode distance greater than 3.175 mm ($= w / 0.8$). The actual parameters of the two-dimensional PSD are:

$$d = 3.2 \text{ mm} ,$$

$$w = 2.54 \text{ mm} ,$$

$$s = 1.0 \text{ mm} ,$$

$$\text{active area (= window) : } 100 \times 100 \text{ mm}^2 .$$

As shown in Fig. 07, the X&Y strips are connected to the cells of delay lines. Each absorbed photon generates two pairs of signals at the ends of the

delay lines, from which the photon (X,Y) position is estimated after the signal processing described in Section 2.3.

3.3 Wire Weaving

The anode wire plane is an electrode of delicate construction. It should be noted that the wires must all be at the same regular pitch, in the same plane, under the same mechanical tension. These requirements could hardly be met in a simple manual construction.

A wire weaving machine has been developed to build wire frames in an algorithmic way, controlled from a computer interface. It consists in two stepping motors driving the wire in two orthogonal directions. A wire spool is fixed to a support where a DC motor unwinds the wire on the X&Y plane, under constant mechanical tension.

While the stepping motors carry the wire in a zig-zag motion over a surface of programmed size, the wire is regularly bind to guide pins placed along the X direction. The pins are precisely fixed at 1 mm pitch, and are all rectified to the same height, thus guaranteeing the wire to be weaved in regular pitch and in the same plane.

Once a wire frame has been weaved, it is soldered to a printed circuit board support that constitutes the anode. The machine weaves gold coated tungsten wires of diameters as small as 6 μm .

3.4 Data Acquisition System

Since the delay line method is used to read both coordinates of the photon position, the electronic parts involved in the Data Acquisition System for the two-dimensional PSD are similar to those described in Section 2.3. One group of electronic modules (pre-amplifiers, amplifiers & discriminators, external delay, time to analog converter and ADC) is required for each coordinate. However, a further step must be added in the two-dimensional Data Acquisition System in order to join together the X&Y digital words corresponding to the coordinates of each event (absorption of a photon), and to histogram and display spectra in two dimensions.

Since photons may be randomly absorbed in the detecting medium, some care must be taken not to mix up the coordinates of different events. One criterium for avoiding this mixture consists in using the anode avalanche pulse to trigger a logic gate of definite width in time. The width is pre-set to be of the same magnitude as the total delay time of the delay line, so that, for each detected photon, the logic gate enables the X&Y conversion during the pre-set

time interval. Since the gate is triggered by the anode signal, the two (and only two) 'start-stop' pairs of pulses coming from the X&Y delay lines must necessarily occur during the gate interval. In case of occurrence of more (or less) than two pairs of 'start-stop' pulses during the gate, the event must be rejected for corresponding to ambiguous data conversion. This is the case when a photon is absorbed before the coordinates of the precedent photon is recorded.

The probability for two photons to be absorbed in the detector within a time interval smaller than the total delay time of the delay line (that is, almost simultaneously) increases with the delay time and with the rate of arrival of photons in the detector. This means that 'fast' delay lines should be provided in detectors supporting high counting rates. However, since the counting rate is limited to $\approx 10^8$ counts/second due to other parts of the data processing (time to analog and analog to digital conversion), delay times smaller than 10^{-6} s do not contribute critically to limitations in the counting rate of the detector.

IV - CHARACTERISATION MEASUREMENTS

The performance of a PSD may be characterised by specific measurements which show the important parameters to be taken into account when the detector is used in a defined application [6]. We describe below some of these measurements and the associated characterisation parameters. It must be noted that the results of these measurements refer not only to the detector but to the whole detection system, including the electronic parts mentioned in Section 2.3. As far as these electronic parts are well adjusted to the role they play in the the detection system, so far the characterisation measurements show the detector individual performance.

4.1 - Spatial Resolution (RES): If the detector were exposed to an infinitely narrow beam of photons, the PSD response would present a finite width. The response is visualized as a plot of *Number of Counts x Position*, which may be interpreted as the experimental points of a mathematical function called "point-spread function". The full width at half maximum (FWHM) of this function is the parameter characterising the detector spatial resolution. In fact, since a beam of photons is never 'infinitely narrow', the point-spread function (f) may not be perfectly measured. The experimental data (e) represent the convolution of the true beam (g) by 'f':

$$e = f \cdot g .$$

The shape of the beam profile and the point-spread function are usually fitted by gaussian functions. In this case, the experimental data are also fitted by a gaussian of FWHM given by:

$$[FWHM]_{measured} = \sqrt{RES^2 + \Delta^2} ,$$

where RES (\approx spatial resolution of the detector) and Δ (\approx width of the photon beam) are respectively the FWHM for the point-spread function and for the beam profile. This is a practical relation from which one may estimate the spatial resolution.

In Fig. 08 is shown the spectrum obtained for the illumination (by an Fe^{55} X-Ray source) of a 50 μm slit placed close to the window of a one-dimensional PSD. The FWHM of the measured spectrum is 0.312 mm. From the considerations above we estimate the spatial resolution of the detector: $RES \approx 300 \mu m$.

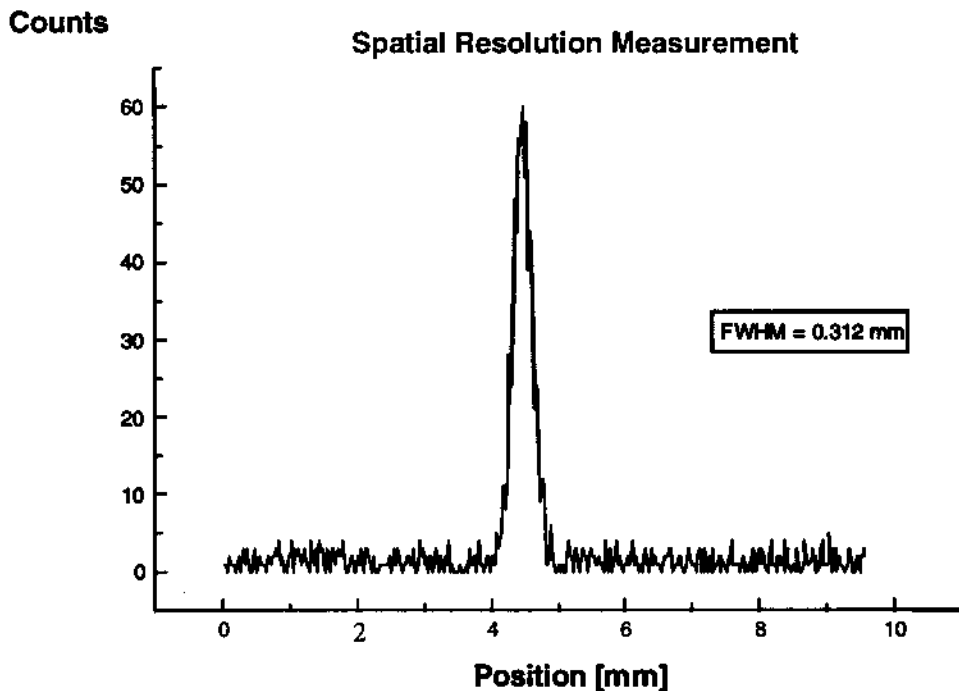


Fig. 08: Detector response for a 50 μm wide slit.

4.2 - Linearity (LIN): A linear relation is expected to exist between the actual position of incidence of photons and the position measurement provided by the detection system. In the case of the detectors here described, the linearity measurement mainly evaluates the quality of the delay line. The time taken for the avalanche signal to travel from the incidence position until the extremities of the delay line is the essential measurement done by the detection system. Irregularities in the delay line construction may introduce linearity losses.

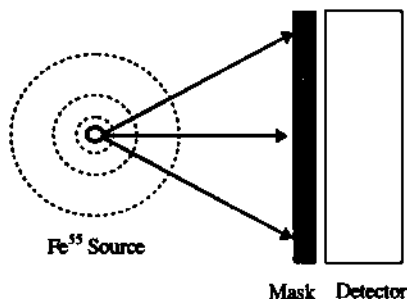


Fig. 09: Overview of the linearity measurement setup.

In order to evaluate the detector linearity, a simple technique consists in providing a mask containing regularly spaced slits. The mask is placed upon the detector window as it is illuminated by an isotropic X-Ray emitting source (See Fig. 09). Photons passing through the slits are counted by the detector and a set of peaks should be measured by the detection system, corresponding to the positions of the slits in the mask. Fig. 10 shows a spectrum obtained with one such mask. The slits are 300 μm wide, 8 mm long, spaced at a pitch of 2 mm.

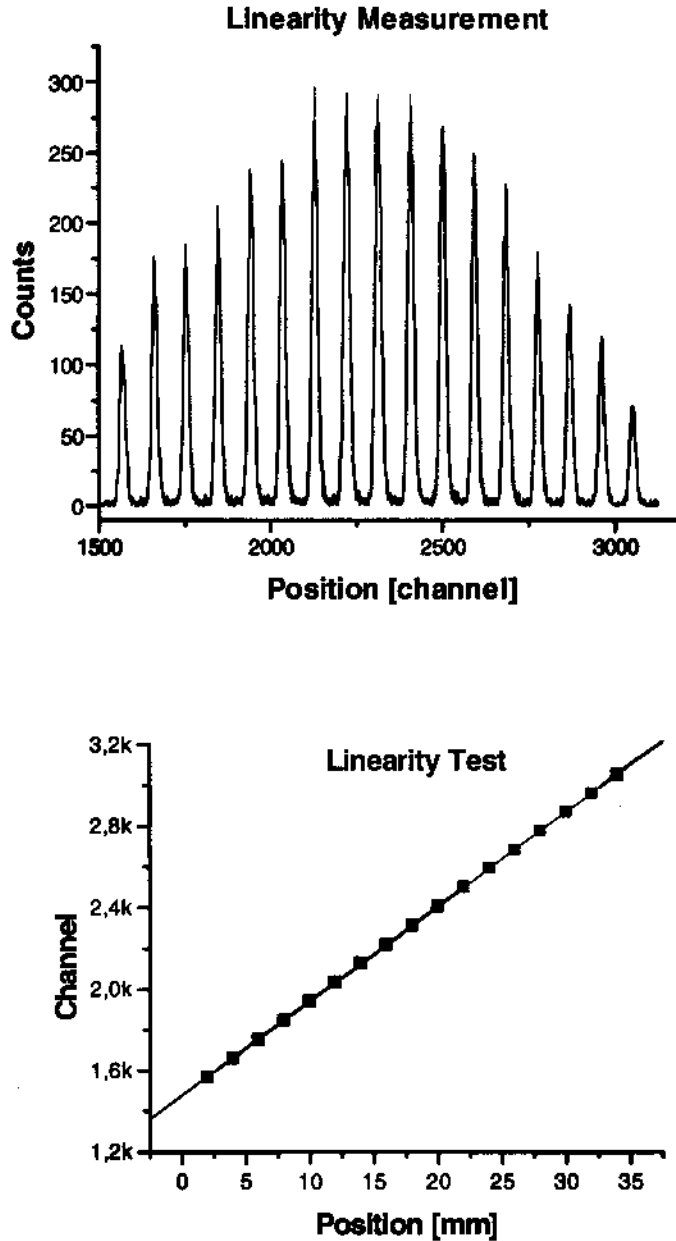


Fig. 10: Upper graph: linearity spectrum obtained with mask. Lower graph: plot of *true x measured* position , with line fit to data.

Due to the finite distance from detector to source, and to the length of the slits, we note that the amplitude of the peaks decreases from the center to the edges of the illuminated region. In the lower graph of Fig. 10, a line has been fitted to the plot of channel number x incidence position. The maximum deviation of the measured channel number with respect to the line fit is below 0.1% of the active length of the detector. This is the usual parameter evaluating the detector linearity. In the case illustrated by Fig. 10: $LIN < 0.1\%$.

4.3 - Homogeneity (HMG): When the active window of a PSD is illuminated with a homogeneous and isotropic X-Ray emitting source, a

corresponding homogeneous response of the detector is expected. The homogeneity measurement evaluates the overall detecting efficiency of the detector. The quantum nature of a photon source implies that an average emission rate of N photons/second exhibits a statistic fluctuation,

$$\Delta N = \frac{1}{\sqrt{N}}$$

This relation is obtained when one considers the photon emission as a Poisson process. Thus, if every pixel of a PSD is hit by an average number of N photons per second, a minimum error of $\pm \Delta N$ is present in the counting response of each pixel. Absolute errors exceeding ΔN are in principle due to the detecting system. A homogeneity spectrum (Number of counts per unit time \times position) exhibits global and localized problems in the detector efficiency. It may be considered as a generalized linearity spectrum. This is why the parameter (HMG) describing the homogeneity is also called 'differential non-linearity'. In the case of uniform illumination of the active window of a PSD, HMG is defined as the maximum deviation of the measured number of counts per pixel relatively to the average number, N_{avg} , of counts over all detecting pixels (= channels). Clearly, if N_{avg} is a high number, the statistic fluctuation is negligible and non-homogeneities are more easily observed.

The experimental setup for measuring homogeneity is similar to the one shown in Fig. 09, with the difference that the X-Ray source is placed as far as possible from the detecting window - in order to assure a 'flat' illumination - and no mask is present in front of the detector.

In Fig. 11 is shown a homogeneity spectrum featuring an average number of 1158 counts per channel. The intrinsic statistic error is about 3%. Except at the ends of the spectrum, where the extremities of the anode wire contribute, most of the encoded number of counts over all the channels is roughly within the statistic fluctuation. No strong deviations with respect to the average number of counts are observed in the spectrum, indicating that HMG is somewhat close to 3%. In order to evaluate HMG more precisely, a higher counting statistics is required.

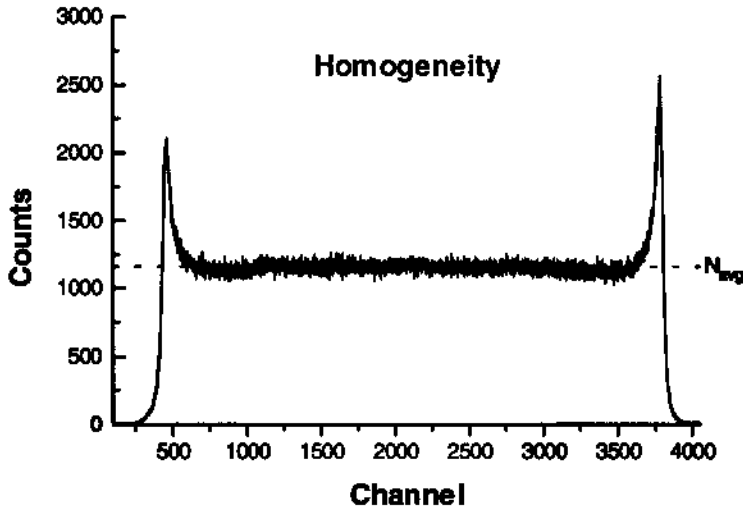


Fig. 11: Homogeneity spectrum with relatively poor counting statistics

Fig. 12 is a series of homogeneity spectra, where each graph shows the accumulated spectrum after 1000 seconds exposition time. We notice that irregularities in the detector response appear gradually as the counting statistics increase.

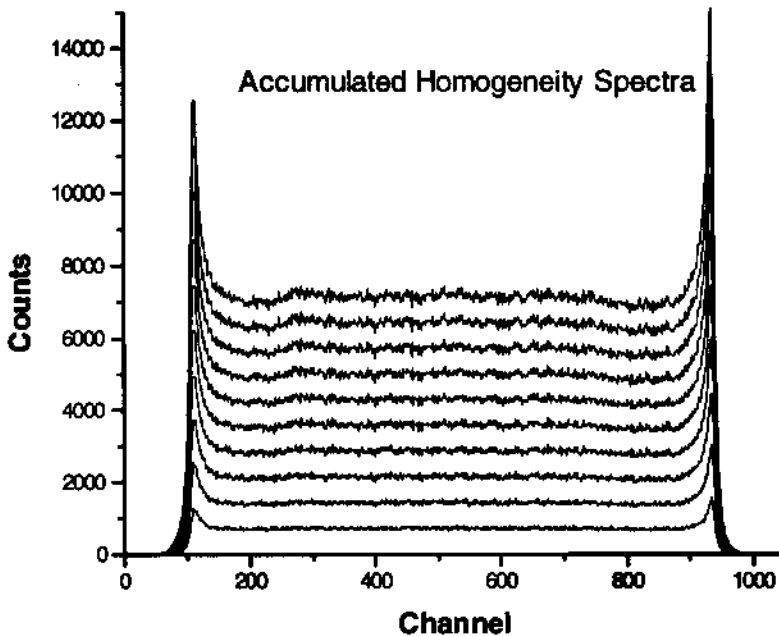


Fig. 12: Series of 10 homogeneity spectra, each one recorded after 1000 seconds data acquisition time.

The photon absorption efficiency of the gas and of the material composing the detector window contribute to the homogeneity of a detector, but normally they do not add localized irregularities. These are generally introduced by dust or grease present in the electrodes, as well as by factors external to the detector (eg. impedance matching of electronic modules, electromagnetic interference, etc.).

In Fig. 13 is shown a homogeneity spectrum with high counting statistics (ΔN less than 1%). Excluding the regions close to the extremities of the spectrum and computing the average number N_{avg} of counts per channel, we note that the region between channels 200 and 400 presents the maximum deviation with respect to the average. Fig. 14 shows a close view of this region, taken from a spectrum where the statistical fluctuation is less than 0.7%. From this one can evaluate the homogeneity parameter for the detector: $HMG < 4\%$.

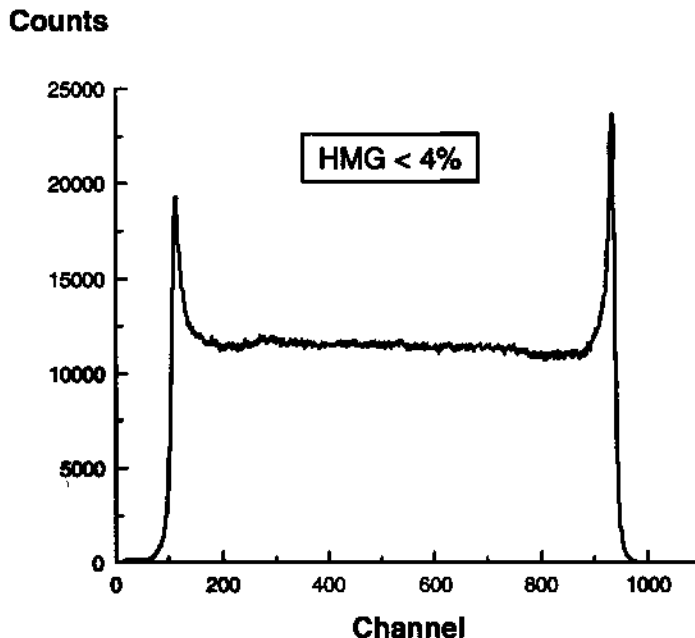


Fig. 13: Homogeneity spectrum with high counting statistics

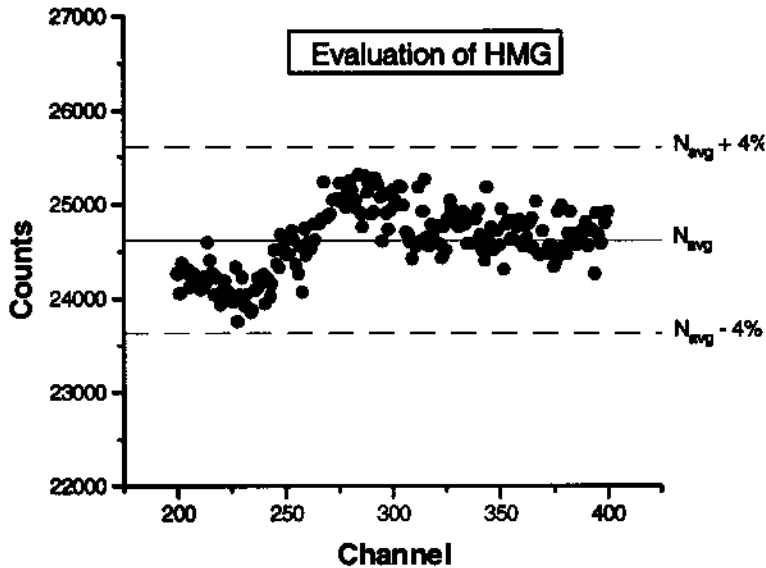


Fig. 14: Evaluation of the HMG parameter for the spectrum shown in Fig. 13.

V - CONCLUSION

The use of a delay line in the measurement of the position of X-Ray photons from the propagation time of electric pulses in a gas detector is quite effective. Only two channels ("start" and "stop") of electronic signal processing are required, independently of the active region of the detector. The amount of electronic modules necessary in the data acquisition is thus relatively small, constituting a low cost detection system for real-time operation under high counting rates ($\approx 10^5$ photons per second).

The Linear Position Sensitive Detectors + Pre-Amplifiers built at CBPF exhibit position resolution of $\approx 300 \mu\text{m}$, linearity better than 0.1% and homogeneity $< 4\%$. These features are fairly comparable to commercially available detectors using delay lines to encode the position of the absorbed photons. A two-dimensional detector is under development and should be commissioned in the near future.

VI - ACKNOWLEDGEMENTS

We are grateful to the directories of CBPF and LNLS (National Synchrotron Light Source), respectively for the implementation of the Detectors Laboratory, and for the support on several practical aspects of the development of the detectors. We also thank Ana Lúcia Capechi (Scientific Initiation Student) for the participation in the construction of delay lines and pre-amplifiers.

VII - REFERENCES

- [1] - A. Gabriel. *Rev Sci. Instr.*, **48**, 10, 1303 (1980).
- [2] - D. H. Wilkinson, *Ionization Chambers and Counters*, Cambridge University Press, (1950).
- [3] - G. Charpak, T. Bouclier, T. Bressani. *Nucl. Instrum and Meth.* **62**, 235 (1968).
- [4] - A. F. Barbosa. PhD Thesis. Université Joseph Fourier/Grenoble (1992).
- [5] - G. C. Smith, B. Yu, J. Fischer, V. Radeka, J. A. Harder. *Nucl. Instrum. and Meth.* **A323**, 78 (1992).
- [6] - U. W. Arndt. *Jour. Appl. Cryst.*, **19**, 145 (1986).